Nanotechnology **22** (2011) 245103 (8pp) doi:10.1088/0957-4484/22/24/245103

Non-vanishing ponderomotive AC electrophoretic effect for particle trapping

Weihua Guan[1], **Jae Hyun Park**[2], **Predrag S Krstić**[2] and **Mark A Reed**[1,3]

[1] Department of Electrical Engineering, Yale University, New Haven, CT 06520, USA
[2] Physics Division, Oak Ridge National Laboratory, Oak Ridge, TN 37831, USA
[3] Applied Physics, Yale University, New Haven, CT 06520, USA

E-mail: mark.reed@yale.edu

Received 8 February 2011
Published 21 April 2011
Online at stacks.iop.org/Nano/22/245103

Abstract

We present here a study on overlooked aspects of alternating current (AC) electrokinetics—AC electrophoretic (ACEP) phenomena. The dynamics of a particle with both polarizability and net charges in a non-uniform AC electric trapping field is investigated. It is found that either electrophoretic (EP) or dielectrophoretic (DEP) effects can dominate the trapping dynamics, depending on experimental conditions. A dimensionless parameter γ is developed to predict the relative strength of EP and DEP effects in a quadrupole AC field. An ACEP trap is feasible for charged particles in 'salt-free' or low salt concentration solutions. In contrast to DEP traps, an ACEP trap favors the downscaling of the particle size.

(Some figures in this article are in colour only in the electronic version)

1. Introduction

Dielectrophoretic (DEP) traps have been successfully implemented for many applications [1–3]. Such traps operate through the interaction of induced polarization charges with non-uniform electric fields. According to the classic DEP theory [4], the sign associated with the real part of the Clausius–Mossotti (CM) factor ($K(\omega)$, figure 1(a)) dictates the behavior of the particle. For $\mathrm{Re}[K(\omega)] > 0$, particles will be directed towards a local electric field maxima (positive DEP, pDEP), while for $\mathrm{Re}[K(\omega)] < 0$, the particle is attracted to a local electric field minima (negative DEP, nDEP). Negative DEP traps offer distinct advantages for many applications since the particles are trapped away from electrodes, mostly with a quadrupole geometry [5–9]. The frequency that produces a change from pDEP to nDEP is referred to as the crossover frequency f_{co} and is given by $(1/2\pi)[(\sigma_{\mathrm{p}} - \sigma_{\mathrm{m}})(\sigma_{\mathrm{p}} + 2\sigma_{\mathrm{m}})/(\epsilon_{\mathrm{m}} - \epsilon_{\mathrm{p}})(\epsilon_{\mathrm{p}} + 2\epsilon_{\mathrm{m}})]^{1/2}$ (in Hz, [4]), where σ and ϵ are the conductivity and permittivity, respectively, with p and m denoting the particle and medium. This prediction is in good agreement with experimental data in salt solutions for nanoscale to microscale latex beads [8]. However, we observe in our experiment that the charged polystyrene beads suspended in 'salt-free' deionized (DI) water can be trapped in the center of a quadrupole electric field for frequencies significantly below the predicted crossover frequency (figure 1 and experimental details in appendix A). This 'anomalous' center trapping behavior in the pDEP region (shaded area in figure 1) motivates us to investigate other contributions in the trapping dynamics. The first possible mechanism for this 'anomalous' trapping behavior is AC electro-osmosis (ACEO), which would play a dominant role in the case of low frequencies and low conductivities [10]. Indeed, we observe ACEO in our experiments, but only at frequencies around 1 kHz, far below the frequency regime of consideration here (a lower limit around 20 kHz). As a result, ACEO is not responsible for the anomalous center trapping behavior at frequencies higher than 20 kHz.

It is well known that most polarizable particles and molecules suspended in aqueous solutions will develop surface charges by either dissociation of surface chemical groups or adsorption of ions from the solution [11]. Therefore, when placed in a liquid with a spatially non-uniform electric field, colloidal particles experience not only a dielectrophoretic (DEP) force but also an electrophoretic (EP) force [12–14]. It is a widely held notion that the EP effect in aqueous solution will 'vanish' upon high frequency AC fields due to the linearity of EP with electric field [13–15]. As a result, EP contributions are not taken into account in most of the high frequency electrokinetic experiments [6–9]. However,

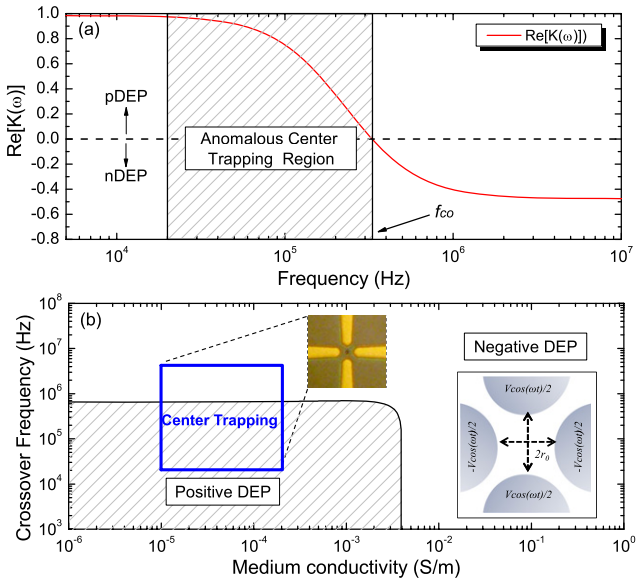

Figure 1. (a) Real part of CM factor (Re[$K(\omega)$]) as a function of the frequency. Shaded area denotes the anomalous center trapping in the theoretical pDEP region. (b) Plot showing the range of the medium conductivity and frequency over which a homogeneous neutral particle experiences nDEP or pDEP. The parameters used in the calculation are $\epsilon_m = 78\epsilon_0$, $\sigma_m = 0.1$–$2\ \mu$S cm^{-1} (measured value), $\epsilon_p = 2.55\epsilon_0$, $\sigma_p = \sigma_{pbulk} + 2K_s/a$, $\sigma_{pbulk} = 0$ S, $K_s = 1$ nS and $a = 500$ nm. The blue box shows the experimental range for successful trapping of a single polystyrene bead in the center of a quadrupole trapping device, schematically shown in the inset ($2r_0$ is the shortest distance between two non-adjacent electrode surfaces). The range of medium conductivities is due to measured variations during the course of the experiments.

the assumption that EP effects will vanish is only true for a spatially homogeneous AC field. A charged particle exposed to an oscillating inhomogeneous electric field can experience a cycle-averaged force. This so-called ponderomotive force [16] plays a significant role in a variety of physical systems such as Paul traps [17] and laser-based particle acceleration [18].

Here we show both experimentally and theoretically the non-vanishing ponderomotive EP effect in high frequency electric field and its application for trapping charged particles in aqueous solutions. In contrast to DEP traps [5–9], an AC electrophoretic (ACEP) would favor the downscaling of the particle size.

2. Theory

We start our analysis with the one-dimensional EP motion of a homogeneous spherical particle with mass m, charge Q and radius a in a high frequency AC electric field. The damping force due to the viscosity of the liquid is of the form $-\xi\dot{x}$, where the Stokes drag coefficient ξ can be approximated by $\xi = 6\pi\eta a$, and η is the dynamic viscosity. Here we assume that the hydrodynamic memory effect [19] can be neglected for the dragging force (i.e. the friction force is only dependent on the current velocity). Without loss of generality, we assume the particle moves in an electric potential consisting of two parts: a static part $U(x)$ and a harmonically oscillating part $V(x)\cos\omega t$, where ω is the angular frequency. The magnitude of $V(x)$ is not assumed small in comparison with $U(x)$. Note that both potentials have a spatial dependence. This potential gives a static force $F(x) = -Q\frac{\partial}{\partial x}U(x)$ and an oscillating force $f(x,t) = QE_0(x)\cos\omega t$, where $E_0(x) = -\frac{\partial}{\partial x}V(x)$.

Under the conditions considered in this paper, the dynamics of the particle can be described by a secular motion $S(t)$ on a timescale typically longer than one oscillating cycle $\tau = 2\pi/\omega$, which is decoupled from the rapidly oscillating micromotion $R(S,t)$ (appendix B). Therefore, the particle motion can be written in the form, $X(t) = S(t) + R(S,t)$, with the constraint $\langle R(S,t)\rangle = 0$ (bracket denotes time-averaging). If the amplitude of the rapidly oscillating motion is much smaller than the characteristic length of the non-uniform electric field $E_0/\frac{\partial E_0}{\partial x}$ (i.e. $2Q\frac{\partial E_0}{\partial x} \ll m\omega^2$), it is reasonable to assume $|S| \gg |R|$ (where the dependence on t and S are henceforth dropped for brevity). Therefore R can be considered a small perturbation to S, and thus the equation of motion, $m\ddot{X} = -\xi\dot{X} + F(X) + f(X,t)$, can be expanded to the first order in R:

$$m(\ddot{S} + \ddot{R}) = -\xi(\dot{S} + \dot{R}) + F(S) + f(S,t) + R\frac{\partial}{\partial x}(F(x) + f(x,t))|_{x=S}. \quad (1)$$

The rapidly oscillating terms on each side of equation (1) must be approximately equal, $m\ddot{R} \approx -\xi\dot{R} + f(S,t)$. The oscillating term $R\frac{\partial F(x)}{\partial x}$ is neglected by assuming $\xi\omega \gg \frac{\partial F(x)}{\partial x}$, which is reasonable for highly damped environments such as water. By integration, we obtain the rapid micromotion component as

$$R(S,t) \approx -\frac{f_0(S)}{m\omega^2[1 + (\xi/m\omega)^2]}\left(\cos\omega t - \frac{\xi}{m\omega}\sin\omega t\right) \quad (2)$$

where $f_0(x) = QE_0(x)$. The rapid micromotion $R(S,t)$ is thus an oscillation at the same frequency as $f(x,t)$. The oscillating amplitude depends on the position of the secular motion through $f_0(S)$, the driving frequency, the damping coefficient and the particle mass.

The secular motion $S(t)$ can therefore be found by averaging equation (1) over one period of the rapid micromotion, and by replacing $f_0(x)$ with $QE_0(x)$:

$$m\ddot{S} = -\xi\dot{S} + F(S) - \frac{Q^2E_0(x)\frac{\partial E_0(x)}{\partial x}|_{x=S}}{2m\omega^2[1 + (\xi/m\omega)^2]}. \quad (3)$$

It should be noted that the above analysis is valid for any viscosity of the medium when $\omega \gg \sqrt{2Q\frac{\partial E_0}{\partial x}/m}$ (appendix B). This inequality is valid for most experiments [6–9] performed in an aqueous environment around the MHz range.

Let us consider three related cases based on equation (3).

Case I, uniform AC electric field with no DC component ($\frac{\partial}{\partial x}E_0(x) = 0$, *and* $F(S) = 0$). Under this circumstance, the averaged secular motion is described by $m\ddot{S} = -\xi\dot{S}$. By integration, we obtain $S = A_1e^{-\xi t/m} + A_2$, where A_1 and A_2 are constants depending on initial conditions. This is simply a transient response and will not contribute to a long timescale drift motion. Since the amplitude of the

superimposed rapid micromotion $R(S,t)$ is usually negligible at high frequency ($\sim 1/\omega^2$, equation (2)), high frequency ACEP effects vanish in this case. This is consistent with O'Brien's results with a parallel plate geometry [20]. Note that O'Brien assumed a uniform electric field. It is thus invalid to apply O'Brien's result directly for the cases of non-uniform electric fields [21, 22].

Case II, non-uniform AC electric field with no DC component ($\frac{\partial}{\partial x}E_0(x) \neq 0$, *and* $F(S) = 0$). The third term on the right-hand side of equation (3) provides a ponderomotive EP force for the secular motion due to the non-uniformity of the electric field. The particle is directed towards a point with a weaker electric field. Moreover, due to the squared dependence on charge Q in equation (3), the repelling of the particle from regions of high electric field intensity holds true for both positive and negative charges. We need to emphasize that, even though the time average over one period of both $f(S,t)$ and $R(S,t)$ is zero at a fixed point, averaging over the micromotion in the non-uniform electric field is the essential mechanism that causes the movement of charged particles.

Case III, non-uniform AC electric field with DC component ($\frac{\partial}{\partial x}E_0(x) \neq 0$, *and* $F(S) \neq 0$). In this case, it is convenient to express $F(x)$ and $E_0(x)$ in equation (3) by potential energy derivatives and the motion equation is obtained as $m\ddot{S} = -\xi\dot{S} - Q\frac{\partial}{\partial x}(U(x) + \Phi_{sp}(x))|_{x=S}$, where $\Phi_{sp}(x)$ defines an AC pseudopotential, which is given by

$$\Phi_{sp}(x) = \frac{QE_0^2(x)}{4m\omega^2[1 + (\xi/m\omega)^2]}. \tag{4}$$

As a consequence, the particles will move towards a point where $\frac{\partial}{\partial x}(U(x) + \Phi_{sp}(x)) = 0$ and oscillate there, which is described by equation (2). In other words, under this situation the charged particle will oscillate at the bottom of the effective pseudopotential. Since $f_0(S)$ is a complex function of time, the motion towards and around the bottom of the effective pseudopotential depends on the detailed form of $E_0(x)$, and other parameters of the system (frequency ω, viscosity ξ, etc).

To this end, we have investigated in detail the EP behavior of a charged particle in a high frequency ($\omega \gg \sqrt{2Q\frac{\partial E_0}{\partial x}/m}$) AC electric field. A translational motion is unarguably possible for charged particles in a non-uniform AC field. As a result, simply ignoring the EP effect in the AC trapping field may not be correct.

3. Relative contributions of DEP and EP effects

Taking the EP effect into consideration for the quadrupole trapping field shown in the inset to figure 1(b), the total instantaneous force on the particle will be $m\ddot{r} - \xi\dot{r} + F_{ep} + F_{dep} = 0$, where F_{ep} and F_{dep} are the instantaneous EP force and instantaneous DEP force, respectively. Although analytical solutions for a general case cannot be obtained, information about the relative contribution of EP and DEP to the trapping dynamics can be obtained from a ponderomotive force point of view, which could give a more intuitive insight. The ponderomotive force for DEP effect is well studied [4, 11] and has the form $\langle F_{dep}\rangle = \pi\epsilon_m a^3 \mathrm{Re}[K(\omega)]\nabla E_0^2(\vec{r})$ in the point dipole approximation. We note that this point dipole approximation gives an upper bound to the DEP force [23]. The ponderomotive force for the EP effect can be expressed as $\langle F_{ep}\rangle = -Q^2\nabla E_0^2(\vec{r})/[4m\omega^2(1 + (\xi/m\omega)^2)]$ for the AC-only case. As a result, spatial non-uniformity of the electric field (aforementioned cases II and III) is critical for both DEP and EP ponderomotive forces.

The ratio of the EP versus the DEP ponderomotive force will determine the dominant mechanism. For arbitrarily complex trap geometries or potentials, this requires a case-by-case numerical calculation. We here choose a symmetric geometry for illustrative purposes, which is a good approximation to many experimentally realized traps [5–9]. Assuming a quadrupole AC electric potential $\varphi(x,y,t) = V\cos(\omega t)(x^2 - y^2)/2r_0^2$ (note that we have considered the one-dimensional motion without loss of generality. Namely, in the case of a quadrupole trap the motions of a particle are independent in each dimension), the ponderomotive force for both DEP and EP can be written as $\langle F_{dep}\rangle = -k_{dep}\vec{r}$ and $\langle F_{ep}\rangle = -k_{ep}\vec{r}$, where k_{dep} and k_{ep} (defined as the trap stiffness for EP and DEP effect) are of the forms

$$k_{dep} = -\mathrm{Re}[K(\omega)]\frac{2\pi\epsilon_m a^3 V^2}{r_0^4} \tag{5}$$

$$k_{ep} = \frac{Q^2V^2}{2m\omega^2 r_0^4[1 + (\xi/m\omega)^2]}. \tag{6}$$

In order to hold the particle in the center of the trap, the ponderomotive force for both EP and DEP should be a restoring force (i.e. k_{ep} and k_{dep} should be positive). For DEP trapping, this means a negative value of $\mathrm{Re}[K(\omega)]$ is needed (nDEP).

From the above analysis we see that both EP and DEP effects are able to trap the particle in the center of the device. Since the trap stiffness can be experimentally estimated through the equipartition theorem as $k = \kappa_B T/\delta^2$, where κ_B is Boltzmann's constant, T the absolute temperature and δ the thermal fluctuations due to Brownian noise, experiments on extracting the position fluctuations of a trapped particle in 'salt-free' water are performed to examine the dominant mechanism. Figure 2 shows the trap stiffness in both x and y directions as a function of V^2. According to equations (5) and (6), both k_{ep} and k_{dep} have a linear dependence on V^2. We attempted a linear fit with the experimental data for both the EP and DEP cases. Since the real part of the CM factor is bounded within $(-0.5, 1)$ [11], the maximum slope for DEP falls very short of the experimental data (dashed blue line). This indicates that the trapping in our 'salt-free' situation cannot be due to the DEP mechanism. In contrast, a fitting by the EP effect (red line) is achievable and estimates the net charge Q as $8.4 \times 10^4 e$. We note that a significant amount of charge is critical for EP trapping to dominate over DEP trapping, as will be shown below.

To compare the relative strengths of the EP and DEP in trapping behavior, a dimensionless parameter γ is defined as

$$\gamma \equiv \left|\frac{k_{ep}}{k_{dep}}\right| = \frac{Q^2}{4|\mathrm{Re}[K(\omega)]|\pi\epsilon_m a^3 m\omega^2[1 + (\xi/m\omega)^2]}. \tag{7}$$

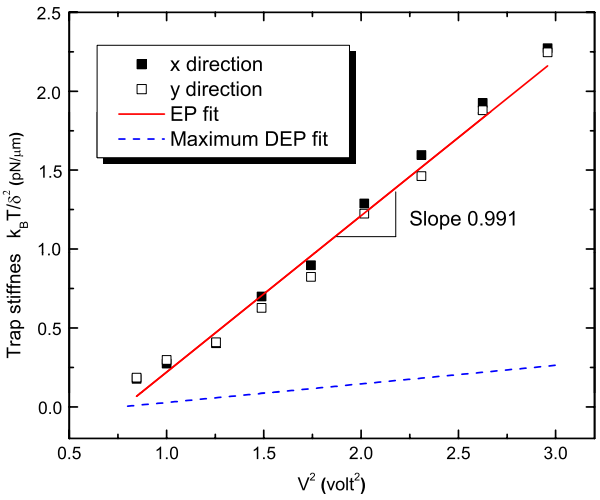

Figure 2. Trap stiffness as a function of the applied AC voltage amplitude squared (V^2) at 3 MHz. The experiment was performed on $a = 240$ nm polystyrene bead in a device with $r_0 = 4$ μm. The squares are the experimental trap stiffness extracted from the position fluctuations in both x and y directions. The dashed blue line is a linear fit with DEP effect by using Re$[K(\omega)]$ as -0.5 (maximum negative value), while the red line is a linear fit with EP effect.

In order for the EP effect to dominate in trapping dynamics, it requires $\gamma \gg 1$. This will happen at a large net charge Q, a small particle size a or a low working frequency ω. Figure 3(a) plots the γ value as a function of Q and a at a fixed frequency (1 MHz), while figure 3(b) shows the γ dependence on Q and ω at a fixed particle size (0.5 μm). It should be emphasized that, even though the γ parameter derived here is based on a quadrupole electric field, the general conclusion holds true for other geometries: the EP effect can dominate the trapping dynamics in the case of a sufficiently high charge in a non-uniform electric field.

4. Discussion

Based on this γ parameter, we are then able to make a consistent explanation for our experiment and other DEP trapping experiments with a quadrupole electric field [6–9]. The key parameter involved is the amount of net charge. Notice that the charge we used in the derivations above is the effective net charge rather than the bare charge [24]. A charged surface in contact with a highly conductive liquid creates an induced electric double layer (EDL). A significant fraction of the particle's charge is neutralized by the strongly bounded counterions in the Stern layer. The charged particle plus the thin Stern layer is further screened by diffusive counterions within a characteristic Debye length λ_D. To determine the effective charge Q_{eff}, we look at the motion of charged particles, which is induced by electrostatic forces, friction and electrophoretic retardation forces. Among them, the electrophoretic retardation force originates from the delayed response of the surrounding ionic atmosphere to the motion of a charged particle. The electrophoretic mobility including this retardation effect can be described by Henry's formula [25]:

$$\mu_E = \frac{2}{3}\frac{\varepsilon\zeta}{\eta} f(\alpha) \tag{8}$$

where $\alpha = a/\lambda_D$ is the ratio of particle radius to the Debye length of the electrolyte solution, ε is the dielectric constant of the electrolyte, ζ is the zeta potential and η is the viscosity of the solution. Ohshima *et al* [26] showed that $f(\alpha)$ is a monotonic increasing function that varies from 1 to 3/2. Since ζ potential can be expressed in Debye–Hückel form [27]:

$$\zeta = \frac{Q_{\text{bare}}}{4\pi\varepsilon a(1 + a/\lambda_D)} \tag{9}$$

where Q_{bare} is the bare charge of a particle. The electrophoretic mobility μ_E can be rewritten as

$$\mu_E = \frac{Q_{\text{bare}}}{6\pi\eta a(1 + a/\lambda_D)} f\left(\frac{a}{\lambda_D}\right). \tag{10}$$

The effective charge of a particle can thus be estimated as

$$Q_{\text{eff}} = \frac{f(a/\lambda_D)}{(1 + a/\lambda_D)} Q_{\text{bare}}. \tag{11}$$

At a high ionic concentration c, the Debye length ($\lambda_D \sim c^{-1/2}$) becomes very small, as a result, $a/\lambda_D \gg 1$ and

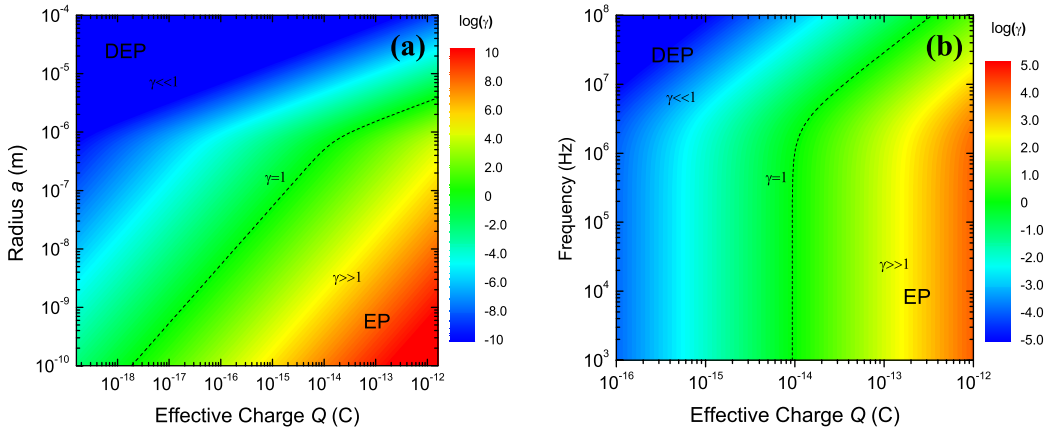

Figure 3. Theoretical plot showing the range of effective net charge Q, particle radius a and working frequency $\omega/2\pi$ over which EP and DEP effects dominate over each other. Note that the color scale is based on $\log(\gamma)$. (a) The γ parameter as a function of Q and a at a fixed frequency (1 MHz). (b) The γ parameter as a function of Q and $\omega/2\pi$ at a fixed particle radius (0.5 μm).

$f(a/\lambda_D) \rightarrow 3/2$. Therefore, $Q_{eff} \approx \frac{3}{2}\frac{\lambda_D}{a} Q_{bare} \ll Q_{bare}$. The effective charge is greatly reduced in salt solutions. This reduced effective charge in high salt concentrations pushes the γ parameter in figure 3 into the DEP dominating region ($\gamma \ll 1$). For most nDEP trapping experiments reported, high salt concentrations were intentionally added to adjust the conductivity of the suspension medium [1, 6–9]. Therefore EP effects in trapping dynamics could be safely neglected for those experiments.

In contrast, it is easy to see from equation (11) that $Q_{eff} \rightarrow Q_{bare}$ when $a \rightarrow 0$ and/or $\lambda_D \rightarrow \infty$. This happens for ultrasmall particles or very low ionic concentrations. For our experiment solutions, $a = 0.5\ \mu$m, $\lambda_D \sim 1\ \mu$m, $Q_{eff} \sim Q_{bare}$. This unscreened large amount of effective charge will direct the γ parameter in figure 3 towards the EP dominating region ($\gamma \gg 1$). An estimation for our 0.5 μm radius beads which showed the 'anomalous' DEP trapping behavior at 20 kHz gives the γ value ~10. Under this circumstance, the EP effect is the dominant mechanism for the center trapping behavior and therefore the predicted pDEP/nDEP boundary becomes invalid (figure 1).

Finally, we briefly comment on the scaling performance of both DEP and EP trap stiffness in the quadrupole trapping device. As shown in equations (5) and (6), reducing the device size r_0 helps to enhance the trapping strength for both EP and DEP in the same fashion ($\sim 1/r_0^4$). Secondly, increasing the applied voltage has the same impact on the trap stiffness ($\sim V^2$) and the maximum voltage that can apply is limited by the breakdown field and other electrokinetic effects (e.g. electrothermal flow [28]). Most importantly, the DEP trap strength decreases with the volume of the particle. Conversely, EP traps prefer smaller particles since the trap stiffness increases with decreasing the mass of the charged particle, which makes the ACEP effect very attractive for single-molecule trapping.

5. Conclusion

In summary, we have elucidated the importance of EP effects in a non-uniform AC electric field. The relative contributions of both DEP and EP effects in a quadrupole trapping field are studied and an important dimensionless parameter γ is obtained, which presents a consistent explanation for both the anomalous trapping behavior in 'salt-free' deionized water and most other DEP trapping experiments with salt solution. EP traps prefer smaller particles, as long as the particles are sufficiently charged. Therefore, it might be feasible to trap single molecules by the EP effect.

Acknowledgment

This research is supported by the US National Human Genome Research Institute of the National Institutes of Health under grant no. 1R21HG004764-01.

Appendix A. Experimental methods

Our planar quadrupole trapping device was fabricated on an SiO_2/Si wafer. The insulating SiO_2 layer has a thickness of 3 μm. Four Au/Cr (~400/50 nm) electrodes were formed on top of this insulating substrate by UV-lithography and a double layer liftoff process. The tip to tip distance ($2r_0$) for each electrode pair ranges from 2 to 8 μm. The microfluidic channel was formed by poly(dimethylsiloxane) (PDMS) using *SU*-8 as a molding master [29]. Oxygen plasma treatment was used to permanently bond the PDMS to the device surface and form an anti-evaporation microfluidic channel. An inlet and an outlet were punched through before assembling. Once the device was assembled, it could be repeatedly used for a long time.

Table A.1. Bead properties.

Diameters (μm)	Parking area (Å^2/group)	Number of −COOH groups[a]	Net charges $Q(e)$[b]
0.481 ± 0.004	158.2	4.59×10^5	8.4×10^4
0.982 ± 0.013	7.9	3.83×10^7	1.8×10^5

[a] By titration method. [b] By fitting method described in main text.

The particles used in the experiments are polystyrene beads (Polysciences, Warrington, PA) of two diameters ($0.481 \pm 0.004\ \mu$m and $0.982 \pm 0.013\ \mu$m). The surface of these particles is functionalized with carboxylate groups (−COOH). The parking area for each group is around 320 Å^2/group. Table A.1 summarizes the properties for these two kinds of beads. These COOH surface groups are the origin of the negative charges (COO^-). Scanning electron microscopy (SEM) revealed that all the particles had a pronounced spherical shape.

The solution used in the experiment was prepared by the following steps: (i) the beads were firstly diluted to a density of ~10^6 particle ml^{-1} by deionized (DI) water (milli-*Q* grade, resistivity 18 MΩ cm), in order to eliminate the particle–particle interactions during the experiment. (ii) In order to thoroughly remove the residual ions from the stock solution, the beads prepared in step 1 were washed five times in DI water by centrifuging the beads in a 10 ml tube at 13 500*g* for 10 min, re-suspending in DI water each time. Salt solutions with 0.1×, 1× and 10× phosphate buffered saline (PBS) (Sigma, St Louis, MO) were also prepared, following the same steps (i) and (ii). The final conductivity of the 'salt-free' solution was measured as 0.1 μS cm^{-1} (EC 215 Multi-range Conductivity Meter, Hanna Instruments) and this slowly goes up to maximum of 2.0 μS cm^{-1} during the course of an experiment (mostly due to the gas absorption).

The particle conductivity is estimated as $\sigma_p = \sigma_{pbulk} + 2K_s/a$, where $\sigma_{pbulk} = 0$ S and $K_s = 1$ nS is the surface conductance, which was confirmed for polystyrene beads from various techniques [30, 31].

The crossover frequency for salt solutions (PBS solutions) obeys the classic DEP theory very well. In contrast, the crossover frequency for 'salt-free' solution is abnormally low (down to around 20 kHz). This abnormal trapping behavior for 'salt-free' solution was repeated for at least five separate experiments with more than one single particle trapping observations per experiment.

The device was wire-bonded and mounted onto a printed circuit board (PCB). Potentials in the form of $U - V\cos\omega t$,

produced by a function generator (Tektronix AFG3252) together with a voltage amplifier (Tabor Electronics, Model 9250), were delivered to the device through 50 Ω BNC cables and monitored by an oscilloscope (Tektronix DPO 4104).

The motion of the charged particle was monitored by an optical microscope (Olympus BX51) and the video was taken by a high-sensitivity digital CCD camera (Olympus DP70) with the highest shutter speed, as fast as 1/44 000 s. We use a particle tracking algorithm which has been described in detail elsewhere [32] to extract the motion fluctuations. The videos were decomposed into frame sequences using the software VirtualDub (http://www.virtualdub.org). The particle tracking was then carried out using the NIH ImageJ platform (http://rsbweb.nih.gov/ij/) with a particle tracking algorithm (https://weeman.inf.ethz.ch/ParticleTracker).

It should be noted that the video-based position extraction method does not measure the instantaneous particle position and has a problem of 'motion blur', which results from time-averaging a signal over a finite integration time (shuttle time or acquisition time) [33]. This will lead to the underestimation of the real variance and overestimation of the trap stiffness for each data point in figure 2 (main text). However, for a fixed optical set-up, the relative relations between each measured variance (the slope) remain unchanged.

Appendix B. Validation of rapid/secular motion separation

Considering a particle of charge Q and mass m and in a quadrupole linear (2D) trap of characteristic radius r_0 and electric potential, $\varphi(x, y, t) = \frac{U - V\cos\omega t}{2r_0^2}(x^2 - y^2)$, which by definition provides a spatially non-uniform electric field, with DC and AC components in the x dimension:

$$\Phi(x,t) = -Q\frac{\partial}{\partial x}\varphi(x,y,t) = -F(x) + f(x,t) \tag{B.1}$$

where

$$F(x) = -m\omega^2\frac{a}{4}x \tag{B.2}$$

$$f(x,t) = m\omega^2\frac{q}{2}x\cos\omega t \tag{B.3}$$

and the trap dimensionless parameters are defined as

$$a = \frac{4QU}{mr_0^2\omega^2} \qquad q = \frac{2QV}{mr_0^2\omega^2}. \tag{B.4}$$

The equation of motion in the x direction is

$$m\ddot{x} = -\xi\dot{x} + F(x) + f(x,t). \tag{B.5}$$

Introducing a dimensionless viscosity b and a dimensionless time τ:

$$b = \frac{2\xi}{m\omega} \qquad \tau = \omega t \tag{B.6}$$

and replacing

$$x = \exp(-b\tau/4)P \tag{B.7}$$

then equation (B.5) takes the form

$$\ddot{P} = hP + \tfrac{1}{2}qP\cos\tau \tag{B.8}$$

where

$$h = \frac{b^2}{16} - \frac{a}{4}. \tag{B.9}$$

Without loss of generality, the solution of equation (B.8) can be written in the form of the Floquet expansion:

$$P(t) = \exp\left(-\mathrm{i}\int_0^\tau \sigma(\tau)\,\mathrm{d}\tau\right)\sum_{n=-\infty}^{\infty} P_n(\tau)\exp(\mathrm{i}n\tau) \tag{B.10}$$

where $P_n(\tau)$ and $\sigma(\tau)$ are slowly varying functions on the timescale such that the external electric field is switched 'on' adiabatically. By equating the same Floquet components and neglecting time derivatives of P_n and σ, the infinite, homogeneous system of equations follows:

$$-n^2P_n - \sigma^2P_n + 2n\sigma P_n = hP_n + \frac{q}{4}(P_{n+1} + P_{n-1}) \tag{B.11}$$

where the dependence on τ is henceforth dropped for brevity and n takes all integers. To secure a nontrivial solution, one equates the infinite tridiagonal determinant of the system with zero. This yields the equation for the infinite number of Floquet–Lyapunov (FL) exponents σ, which define an infinite number of solutions for the system. We will seek the solution for the case of particular experimental interest, $q \ll 1$, under arbitrary dragging parameter b and DC parameter a. Looking for the non-oscillating (P_0) and oscillating terms to the lowest non-vanishing powers in q ($P_{\pm1}$), equation (B.11) simplifies to

$$-\sigma^2P_0 = hP_0 + \frac{q}{4}(P_1 + P_{-1}) \tag{B.12}$$

$$-P_{\pm1} - \sigma^2P_{\pm1} \pm 2\sigma P_{\pm1} = hP_{\pm1} + \frac{q}{4}P_0 \tag{B.13}$$

reducing the infinite homogeneous system into the finite one of order three. Thus

$$P_1 + P_{-1} = -A\frac{q}{2}P_0 + \mathrm{O}(q^2) \tag{B.14}$$

which, when replaced in equation (B.12), gives the FL exponents

$$\sigma_{1,2} = \pm\mathrm{i}\sqrt{h - \frac{A}{8}q^2} = \pm\mathrm{i}\sigma_0 \tag{B.15}$$

where

$$A \approx \frac{1}{1+4h} + \mathrm{O}(q^2). \tag{B.16}$$

Note that the above analysis is valid for an arbitrary drag parameter b and arbitrary DC parameter a. Equation (B.13) yields

$$P_1 = -\frac{q/4}{1 \mp 2\mathrm{i}\sqrt{h}}P_0 \qquad P_{-1} = -\frac{q/4}{1 \pm 2\mathrm{i}\sqrt{h}}P_0. \tag{B.17}$$

Notice that it is easy to show that $P_{\pm2}$ are proportional to q^2, $P_{\pm3}$ to q^3. Therefore $P_{\pm1}$ are the leading coefficients in expansion of small q of the rapid oscillating part of the Floquet expansion in equation (B.10), oscillating with the driving frequency ω. Since in $P_0(t) \sim \exp(\pm\int\sigma_0\,\mathrm{d}\tau)$, σ_0 can be either real or imaginary, the latter case producing secular oscillations of the frequency $\omega\sigma_0$ which is in the limit

$b = 0$, $a = 0$ equal to $\omega q/2\sqrt{2}$, obviously much smaller than ω when $q \ll 1$. However, when $b > 1$ (typical for aqueous environments), $\omega\sigma_0$ is real, and when combined with the exponent in equation (B.7) yields $-(b/4 \mp \sigma_0) < 0$ when $q \ll 1$. This means that $x(t)$ is proportional to an exponentially decreasing function of time, $\exp[-(b/4 \mp \sigma_0)\omega t]$. It is interesting to note that the two exponent factors are quite different in size. Thus, $(b/4 - \sigma_0) \approx \frac{q^2/16}{\sqrt{h}(1+4h)} \ll 1$, while $(b/4 + \sigma_0) \approx b/4 + \sqrt{h} \underset{a\to 0}{\longrightarrow} b/2 \sim 1$. This means only the solution corresponding to σ_1 will define long-time motion in water, the other being a short-time transient.

By neglecting high-order terms in q, we can now write $P(\tau)$ in equation (B.10) as

$$P^{(i)}(\tau) \approx P_0^{(i)} + (P_1^{(i)} \exp(\mathrm{i}\tau) + P_{-1}^{(i)} \exp(-\mathrm{i}\tau)) \tag{B.18}$$

where $i = 1, 2$ correspond to two eigensolutions in equation (B.15):

$$P^{(1,2)} = \left[1 - \frac{q/2}{1+4h}(\cos\omega t \mp 2\sqrt{h}\sin\omega t)\right] \times \exp\left(\pm\omega\int_0^t \sigma_0\,\mathrm{d}t\right). \tag{B.19}$$

The full solution for $x(t)$ is then

$$x(t) = \exp\left(-\frac{b}{4}\omega t\right)(A_1 P^{(1)} + A_2 P^{(2)}) \tag{B.20}$$

where A_1 and A_2 are the integration constants, depending on the initial conditions. If one assumes zero initial velocity at an initial position x_0, as well as adiabatic switching on of the external potential, then for $b \gg q$, the solution takes the form

$$x(t) = \exp[-(b/4 - \sigma_0)\omega t]P^{(1)}x_0. \tag{B.21}$$

When only an AC field is applied ($a = 0$), it follows

$$x(t) = \exp\left(-\frac{q^2/b^2}{1+b^2/4}\omega t\right)\left[1 - \frac{q/2}{1+b^2/4} \times \left(\cos\omega t - \frac{b}{2}\sin\omega t\right)\right]x_0. \tag{B.22}$$

However, when also $b = 0$ (vacuum case)

$$P^{(1,2)} = \left(1 - \frac{q}{2}\cos\omega t\right)\exp\left(\pm\frac{\omega}{2\sqrt{2}}\int_0^t q\,\mathrm{d}t\right) \tag{B.23}$$

which yields

$$x(t) = x_0\left(1 - \frac{q}{2}\cos\omega t\right)\cos\left(\frac{\omega}{2\sqrt{2}}\int_0^t q\,\mathrm{d}t\right) \tag{B.24}$$

defining the secular angular frequency $\frac{q}{2\sqrt{2}}\omega$.

To make a connection of these results with the more general case of non-uniform electric field in the main text, it can be seen from equations (B.3) and (B.4) that $q = 2Q\frac{\partial E_0(x)}{\partial x}/(m\omega^2)$, where in the case of a quadrupole field, $E_0(x) = Vx/r_0^2$. By the same token, $f_0(S)/(m\omega^2)$ in equation (2) in the main text takes the form $qS/2$ in the case of a quadrupole field. Equation (3) in the main text takes the form

$$m\ddot{S} = -m\omega\frac{b}{2}\dot{S} - m\omega^2\frac{a}{4}S - m\omega^2\frac{q^2/8}{1+4h}S \tag{B.25}$$

where the last term at the right-hand side of equation (B.25) defines the ponderomotive potential for the case of a quadrupole AC potential, yielding the 'simplest' spatially inhomogeneous potential, linear in x.

The harmonic EP pseudopotential of equation (4) in the main text can be written as

$$\Phi_{\mathrm{sp}}(x) \approx \frac{q/8}{1+4h}\frac{V}{r_0^2}x^2. \tag{B.26}$$

Finally, the EP 'trap stiffness' for a linear quadrupole trap has the form

$$k_{\mathrm{ep}} = m\omega^2\frac{q^2/8}{1+4h}. \tag{B.27}$$

References

[1] Fiedler S, Shirley S G, Schnelle T and Fuhr G 1998 Dielectrophoretic sorting of particles and cells in a microsystem *Anal. Chem.* **70** 1909–15

[2] Holzel R, Calander N, Chiragwandi Z, Willander M and Bier F F 2005 Trapping single molecules by dielectrophoresis *Phys. Rev. Lett.* **95** 128102

[3] Chiou P Y, Ohta A T and Wu M C 2005 Massively parallel manipulation of single cells and microparticles using optical images *Nature* **436** 370–2

[4] Pohl H A 1978 *Dielectrophoresis: The Behavior of Neutral Matter in Nonuniform Electric Fields* (Cambridge: Cambridge University Press)

[5] Huang Y and Pethig R 1991 Electrode design for negative dielectrophoresis *Meas. Sci. Technol.* **2** 1142–6

[6] Muller T, Gerardino A, Schnelle T, Shirley S G, Bordoni F, DeGasperis G, Leoni R and Fuhr G 1996 Trapping of micrometre and sub-micrometre particles by high-frequency electric fields and hydrodynamic forces *J. Phys. D: Appl. Phys.* **29** 340–9

[7] Hughes M P and Morgan H 1998 Dielectrophoretic trapping of single sub-micrometre scale bioparticles *J. Phys. D: Appl. Phys.* **31** 2205–10

[8] Green N G and Morgan H 1999 Dielectrophoresis of submicrometer latex spheres. 1. Experimental results *J. Phys. Chem.* B **103** 41–50

[9] Voldman J, Braff R A, Toner M, Gray M L and Schmidt M A 2001 Holding forces of single-particle dielectrophoretic traps *Biophys. J.* **80** 531–41

[10] Bazant M Z and Squires T M 2004 Induced-charge electrokinetic phenomena: theory and microfluidic applications *Phys. Rev. Lett.* **92** 066101

[11] Morgan H and Green N G 2002 *AC Electrokinetic: Colloids and Nanoparticles* (Hertfordshire: Research Studies Press)

[12] Srivastava A K, Kim M, Kim S M, Kim M-K, Lee K, Lee Y H, Lee M-H and Lee S H 2009 Dielectrophoretic and electrophoretic force analysis of colloidal fullerenes in a nematic liquid-crystal medium *Phys. Rev.* E **80** 051702

[13] Gascoyne P R C and Vykoukal J 2002 Particle separation by dielectrophoresis *Electrophoresis* **23** 1973–83

[14] Kumar A, Qiu Z, Acrivos A, Khusid B and Jacqmin D 2004 Combined negative dielectrophoresis and phase separation in nondilute suspensions subject to a high-gradient ac electric field *Phys. Rev.* E **69** 021402

[15] Krupke R, Hennrich F, von Löhneysen H and Kappes M M 2003 Separation of metallic from semiconducting single-walled carbon nanotubes *Science* **301** 344–7
[16] Boot H A H and Harvie R B R S 1957 Charged particles in a non-uniform radio-frequency field *Nature* **180** 1187
[17] Paul W 1990 Electromagnetic traps for charged and neutral particles *Rev. Mod. Phys.* **62** 531–40
[18] Eichmann U, Nubbemeyer T, Rottke H and Sandner W 2009 Acceleration of neutral atoms in strong short-pulse laser fields *Nature* **461** 1261–4
[19] Sparling L C, Reichl L E and Sedlak J E 1986 Effect of hydrodynamic memory on dielectric relaxation *Phys. Rev.* A **33** 699–705
[20] O'Brien R W 1988 Electro-acoustic effects in a dilute suspension of spherical-particles *J. Fluid Mech.* **190** 71–86
[21] Bahukudumbi P, Everett W N, Beskok A, Bevan M A, Huff G H, Lagoudas D and Ounaies Z 2007 Colloidal microstructures, transport, and impedance properties within interfacial microelectrodes *Appl. Phys. Lett.* **90** 224102
[22] Park S and Beskok A 2008 Alternating current electrokinetic motion of colloidal particles on interdigitated microelectrodes *Anal. Chem.* **80** 2832–41
[23] Singh P and Aubry N 2005 Trapping force on a finite-sized particle in a dielectrophoretic cage *Phys. Rev.* E **72** 016602
[24] Diehl A and Levin Y 2004 Effective charge of colloidal particles *J. Chem. Phys.* **121** 121000
[25] Henry D C 1931 The cataphoresis of suspended particles. Part i. The equation of cataphoresis *Proc. R. Soc.* A **133** 106–29
[26] Ohshima H, Healy T W and White L R 1983 Approximate analytic expressions for the electrophoretic mobility of spherical colloidal particles and the conductivity of their dilute suspensions *J. Chem. Soc. Faraday Trans.* II **79** 1613–28
[27] Palberg T, Mönch W, Bitzer F, Piazza R and Bellini T 1995 Freezing transition for colloids with adjustable charge: a test of charge renormalization *Phys. Rev. Lett.* **74** 4555–8
[28] Ramos A, Morgan H, Green N G and Castellanos A 1998 Ac electrokinetics: a review of forces in microelectrode structures *J. Phys. D: Appl. Phys.* **31** 2338–53
[29] Duffy D C, McDonald J C, Schueller O J A and Whitesides G M 1998 Rapid prototyping of microfluidic systems in poly(dimethylsiloxane) *Anal. Chem.* **70** 4974–84
[30] Arnold W M, Schwan H P and Zimmermann U 1987 Surface conductance and other properties of latex-particles measured by electrorotation *J. Phys. Chem.* **91** 5093–8
[31] Hughes M P and Morgan H 1999 Dielectrophoretic characterization and separation of antibody coated submicrometer latex spheres *Anal. Chem.* **71** 3441–5
[32] Sbalzarini I F and Koumoutsakos P 2005 Feature point tracking and trajectory analysis for video imaging in cell biology *J. Struct. Biol.* **151** 182–95
[33] Wong W P and Halvorsen K 2006 The effect of integration time on fluctuation measurements: calibrating an optical trap in the presence of motion blur *Opt. Express* **14** 12517–31